

Collider phenomenology of light strange-beauty squarks

Kingman Cheung¹ and Wei-Shu Hou²¹*Department of Physics and NCTS, National Tsing Hua University, Hsinchu, Taiwan, Republic of China*²*Department of Physics, National Taiwan University, Taipei, Taiwan, Republic of China*

(Received 7 April 2004; published 24 August 2004)

Strong mixing between right-handed strange and beauty squarks is a possible solution to the CP violation discrepancy in $B \rightarrow \phi K_S$ decay as recently suggested by the Belle data. In this scenario, thanks to the strong mixing one of the strange-beauty squarks can be as light as 200 GeV, even though the generic supersymmetry scale is at TeV. In this work, we study the production of this light right-handed strange-beauty squark at hadronic colliders and discuss the detection in various decay scenarios. Detection prospect at the Tevatron run II is good for the strange-beauty squark mass up to about 300 GeV.

DOI: 10.1103/PhysRevD.70.035009

PACS number(s): 11.30.Pb, 12.15.Ff, 12.60.Jv, 14.80.Ly

I. INTRODUCTION

Supersymmetry (SUSY) is the leading candidate for physics beyond the standard model (SM), because it provides a weak scale solution to the gauge hierarchy problem as well as a dynamical mechanism for the electroweak symmetry breaking. Usual treatments of SUSY, however, do not address the problem of flavors. The flavor problem consists of the existence of fermion generations, their mass and mixing hierarchies, as well as the existence of CP violation in quark (and now possibly also in neutrino sector) mixings, and probably has origins above the weak scale. In an interesting combination [1] of Abelian flavor symmetry (AFS) and SUSY, it was pointed out [2,3] that a generic feature is the near-maximal $\tilde{s}_R - \tilde{b}_R$ squark mixing. Such a near-maximal mixing allows for one state to be considerably lighter than the squark mass scale \tilde{m} . Such a state, called the strange-beauty squark $\tilde{s}\tilde{b}_1$, carries both s and b flavors, and is bound to impact on $b \rightarrow s$ transitions.

It is remarkable that we may have a hint for new physics in CP violation in $B \rightarrow \phi K_S$ decay, which is a $b \rightarrow s\bar{s}s$ transition. The SM predicts that the mixing-dependent CP violation in this mode, measured in analogous way as the well established CP violation in $B \rightarrow J/\psi K_S$ mode, should yield the same result. The Belle Collaboration, however, has found an opposite sign in the $B \rightarrow \phi K_S$ mode for two consecutive years [4,5]. The current discrepancy with SM prediction stands at a 3.5σ level. The result from the BaBar Collaboration in 2003 is at odds [6] with Belle, but the combined result is still in 2.7σ disagreement with SM expectation. While more data are needed to clarify the situation, it has been pointed out [7] that a light $\tilde{s}\tilde{b}_1$ squark provides all the necessary ingredients to narrow this large discrepancy with SM prediction. It has (1) a large $s-b$ flavor mixing, (2) a (unique) new CP violating phase, and (3) right-handed dynamics. The latter is needed for explaining why similar “wrong-sign” effects are not observed in the modes such as $B \rightarrow K_S \pi^0$ and $\eta' K_S$. These modes yield consistent results as what was measured in $B \rightarrow J/\psi K_S$. A detailed study of various B decays suggested [7] that $m_{\tilde{s}\tilde{b}_1} \sim 200$ GeV and $m_{\tilde{g}} \sim 500$ GeV are needed, while the squark mass scale \tilde{m}

and other SUSY particles can be well above the TeV scale.

It is clear that a squark as light as 200 GeV is of great interest since the Tevatron has a chance of seeing it. One should independently pursue the search for a relatively light $\tilde{s}\tilde{b}_1$ squark, even if the $B \rightarrow \phi K_S$ CP violation discrepancy evaporates in the next few years. We note that a strange-beauty squark, carrying $\sim 50\%$ in strange and beauty flavor, would lead to a weakening of bounds on beauty squark search based on b -tagging. In this work, we study direct strange-beauty squark-pair production, as well as the feed down from gluino-pair production and the associated production of $\tilde{s}\tilde{b}_1$ with a gluino. It turns out that the dominant contribution comes from direct squark-pair production as long as the squark mass is below 300 GeV. However, for squark mass above 300 GeV, the feed down from gluino-pair production with $m_{\tilde{g}} = 500$ GeV becomes important. We also study various decay scenarios of the strange-beauty squarks at the Tevatron, which is of immediate interest. The most interesting decay mode is $\tilde{s}\tilde{b}_1 \rightarrow b/s + \tilde{\chi}_1^0$, which gives rise to a final state of multi- b jets plus large missing energies. The other scenarios considered are the $\tilde{s}\tilde{b}_1$ -LSP and the R -parity violating $\tilde{s}\tilde{b}_1$ decay possibilities.

The organization of the paper is as follows. In Sec. II we recapitulate the features of the model needed for our collider study. We discuss the production of the strange-beauty squark at hadronic machines in Sec. III, and its decay modes and detection in Sec. IV. Conclusion is given in Sec. V.

II. INTERACTIONS

We do not go into the details of the model, but mention that the d flavor is decoupled [3] to evade the most stringent low energy constraints. The generic class of AFS models [1,2] imply a near-maximal $s_R - b_R$ mixing, which is extended to the right-handed squark sector upon invoking SUSY. We focus only on the 2×2 right-handed strange and beauty squarks, which are strongly mixed. The mass matrix is given by

$$\mathcal{L} = -(\tilde{s}_R^* \tilde{b}_R^*) \begin{pmatrix} \tilde{m}_{22}^2 & \tilde{m}_{23}^2 e^{-i\sigma} \\ \tilde{m}_{23}^2 e^{i\sigma} & \tilde{m}_{33}^2 \end{pmatrix} \begin{pmatrix} \tilde{s}_R \\ \tilde{b}_R \end{pmatrix}. \quad (1)$$

Since the mass matrix is hermitian and the phase freedom has already been used for quarks, so there remains only one CP violating phase [2,3,7]. However, for collider studies it is not yet relevant. With the transformation

$$\begin{pmatrix} \tilde{s}_R \\ \tilde{b}_R \end{pmatrix} = R \begin{pmatrix} \tilde{s}b_1 \\ \tilde{s}b_2 \end{pmatrix} = \begin{pmatrix} \cos \theta_m & \sin \theta_m \\ -\sin \theta_m e^{i\sigma} & \cos \theta_m e^{i\sigma} \end{pmatrix} \begin{pmatrix} \tilde{s}b_1 \\ \tilde{s}b_2 \end{pmatrix}, \quad (2)$$

the mass term is diagonalized as

$$\mathcal{L} = -(\tilde{s}b_1^* \tilde{s}b_2^*) \begin{pmatrix} \tilde{m}_1^2 & 0 \\ 0 & \tilde{m}_2^2 \end{pmatrix} \begin{pmatrix} \tilde{s}b_1 \\ \tilde{s}b_2 \end{pmatrix}. \quad (3)$$

The diagonalization matrix R enters the gluino-quark-squark and squark-squark-gluon interactions. Assuming the quarks are already in mass eigenbasis, the relevant gluino-quark-squark interaction in the mass eigenbasis is

$$\begin{aligned} \mathcal{L} = & -\sqrt{2} g_s T_{kj}^a [-\bar{g}_a P_R s_j \tilde{s}b_{1k}^* \cos \theta_m \\ & + \bar{g}_a P_R b_j \tilde{s}b_{1k}^* \sin \theta_m e^{-i\sigma} - \bar{g}_a P_R s_j \tilde{s}b_{2k}^* \sin \theta_m \\ & - \bar{g}_a P_R b_j \tilde{s}b_{2k}^* \cos \theta_m e^{-i\sigma} + \text{H.c.}], \end{aligned} \quad (4)$$

where $P_R = (1 + \gamma^5)/2$, and a, j, k are the color indices for gluinos, quarks and squarks, respectively. The squark-squark-gluon interaction is

$$\begin{aligned} \mathcal{L} = & -i g_s A_\mu^a T_{ij}^a (\tilde{s}b_{1i}^* \vec{\partial}_\mu \tilde{s}b_{1j} + \tilde{s}b_{2i}^* \vec{\partial}_\mu \tilde{s}b_{2j}) \\ & + g_s^2 (T^a T^b)_{ij} A^{a\mu} A_\mu^b (\tilde{s}b_{1i}^* \tilde{s}b_{1j} + \tilde{s}b_{2i}^* \tilde{s}b_{2j}), \end{aligned} \quad (5)$$

where

$$(T^a T^b)_{ij} = \frac{1}{6} \delta_{ab} \delta_{ij} + \frac{1}{2} (d_{abc} + i f_{abc}) T_{ij}^c.$$

The relevant Feynman rules are listed in Fig. 1.

III. PRODUCTION AT HADRONIC MACHINES

We have set the generic SUSY scale at TeV, except for the gluino and the light strange-beauty squark $\tilde{s}b_1$, which could be as light as 500 and 200 GeV, respectively. These masses are still allowed by the squark-gluino search at the Tevatron [8]. In fact, these limits are more forgiving for the present case because $\tilde{s}b_1$ does not decay into b quark 100% of the time.

A. Processes and formulas

The production of the strange-beauty squark can proceed via the following processes.

- (1) $q\bar{q}$ and gg fusion [Figs. 2(a) and 2(b)]

$$q\bar{q}, gg \rightarrow \tilde{s}b_1 \tilde{s}b_1^*. \quad (6)$$

If the initial state is $s\bar{s}$ or $b\bar{b}$, there is an additional

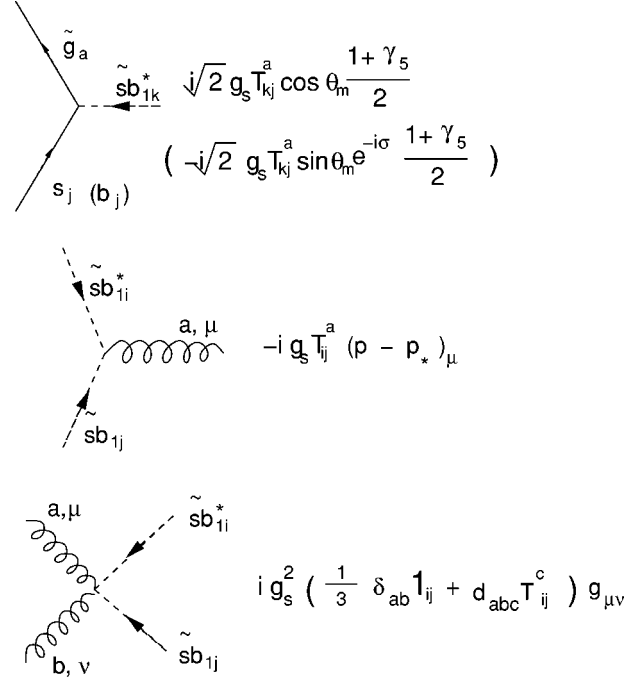


FIG. 1. The relevant Feynman rules used in this work. The momenta are going into the vertex.

contribution from the t -channel gluino exchange diagram, shown in Fig. 2(c). Note that there are also $s\bar{b}, b\bar{s} \rightarrow \tilde{s}b_1 \tilde{s}b_1^*$ contributions via the t -channel gluino exchange diagram only.

- (2) The $ss, bb, \bar{s}\bar{s}, \bar{b}\bar{b}, sb, \bar{s}b$ initial state scattering via t - and u -channel gluino exchange diagrams

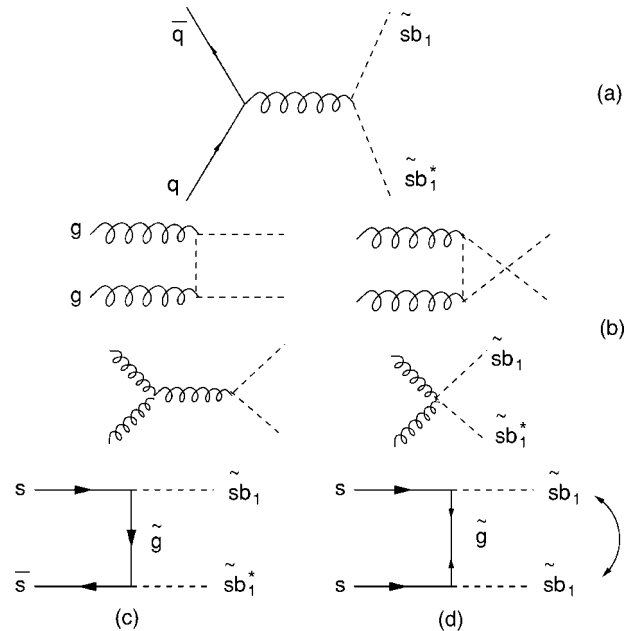


FIG. 2. Contributing Feynman diagrams for (a) $q\bar{q} \rightarrow \tilde{s}b_1 \tilde{s}b_1^*$, (b) $gg \rightarrow \tilde{s}b_1 \tilde{s}b_1^*$, (c) $s\bar{s}(b\bar{b}) \rightarrow \tilde{s}b_1 \tilde{s}b_1^*$, and (d) $ss(bb) \rightarrow \tilde{s}b_1 \tilde{s}b_1^*$.

$$ss, sb, bb \rightarrow \widetilde{s}\widetilde{b}_1\widetilde{s}\widetilde{b}_1^*, \quad \overline{s}\overline{s}, \overline{s}\overline{b}, \overline{b}\overline{b} \rightarrow \widetilde{s}\widetilde{b}_1^*\widetilde{s}\widetilde{b}_1^*, \quad (7)$$

shown in Fig. 2(d).

(3) Gluino pair production, followed by gluino decay,

$$q\bar{q}, gg \rightarrow \widetilde{g}\widetilde{g}; \quad \widetilde{g} \rightarrow s\widetilde{s}\widetilde{b}_1^*, \quad \widetilde{g} \rightarrow b\widetilde{s}\widetilde{b}_1^*, \quad \widetilde{g} \rightarrow s\widetilde{s}\widetilde{b}_1, \quad \widetilde{g} \rightarrow b\widetilde{s}\widetilde{b}_1. \quad (8)$$

For $s\bar{s}$, $b\bar{b}$ in the initial states there are additional t - and u -channel diagrams. Note that $s\bar{b}, \overline{s}\widetilde{b} \rightarrow \widetilde{g}\widetilde{g}$ are also possible through the t - and u -channel diagrams.

(4) Associated production of $\widetilde{s}\widetilde{b}_1$ with gluino

$$sg, bg \rightarrow \widetilde{s}\widetilde{b}_1\widetilde{g}, \quad (9)$$

followed by gluino decay.

Since the gluino has a mass of at least 500 GeV, we expect the t - or u -channel gluino-exchange diagrams to be much smaller than $q\bar{q}$ annihilation diagrams. Moreover, the t - or u -channel gluino-exchange diagrams are only relevant for s or b in the initial state, so the contributions of which are further suppressed by their parton luminosities. Nevertheless, we include all those t -channel gluino diagrams when the initial state quarks are s or b . In gluino-pair production we also keep the t - and u -channel $\widetilde{s}\widetilde{b}_1$ -exchange diagrams for the initial state quarks s or b .

Direct production of $\widetilde{s}\widetilde{b}_1\widetilde{s}\widetilde{b}_1^*$

Let us first introduce some short-hand notation. The $\hat{s}, \hat{t}, \hat{u}$ are the usual Mandelstem variables. We define the following

$$\hat{t}_{\widetilde{g}} = \hat{t} - m_{\widetilde{g}}^2, \quad \hat{u}_{\widetilde{g}} = \hat{u} - m_{\widetilde{g}}^2,$$

$$\hat{t}_{sb} = \hat{t} - m_{\widetilde{s}\widetilde{b}_1}^2, \quad \hat{u}_{sb} = \hat{u} - m_{\widetilde{s}\widetilde{b}_1}^2,$$

$$\beta_{sb} = \sqrt{1 - \frac{4m_{\widetilde{s}\widetilde{b}_1}^2}{\hat{s}}}, \quad \beta_g = \sqrt{1 - \frac{4m_g^2}{\hat{s}}},$$

$$\beta_{sbg} = \sqrt{\left(1 - \frac{m_g^2}{\hat{s}} - \frac{m_{\widetilde{s}\widetilde{b}_1}^2}{\hat{s}}\right)^2 - 4\frac{m_g^2}{\hat{s}}\frac{m_{\widetilde{s}\widetilde{b}_1}^2}{\hat{s}}}.$$

The subprocess cross section for $q\bar{q} \rightarrow \widetilde{s}\widetilde{b}_1\widetilde{s}\widetilde{b}_1^*$ is given by

$$\begin{aligned} & \frac{d\sigma}{d\cos\theta^*}(q\bar{q} \rightarrow \widetilde{s}\widetilde{b}_1\widetilde{s}\widetilde{b}_1^*) \\ &= \frac{2\pi\alpha_s^2}{9\hat{s}}\beta_{sb} \left[\frac{1}{4}(1 - \beta_{sb}^2 \cos^2\theta^*) - \frac{m_{\widetilde{s}\widetilde{b}_1}^2}{\hat{s}} \right], \quad (10) \end{aligned}$$

where θ^* is the central scattering angle in the parton rest frame. Integrating over the scattering angle θ^* , the cross section is given by

$$\sigma(q\bar{q} \rightarrow \widetilde{s}\widetilde{b}_1\widetilde{s}\widetilde{b}_1^*) = \frac{2\pi\alpha_s^2}{27\hat{s}}\beta_{sb}^3. \quad (11)$$

The differential cross section for $gg \rightarrow \widetilde{s}\widetilde{b}_1\widetilde{s}\widetilde{b}_1^*$ is

$$\begin{aligned} & \frac{d\sigma}{d\cos\theta^*}(gg \rightarrow \widetilde{s}\widetilde{b}_1\widetilde{s}\widetilde{b}_1^*) \\ &= \frac{\pi\alpha_s^2}{256\hat{s}}\beta_{sb} \left(\frac{64}{3} - \frac{48\hat{u}_{sb}\hat{t}_{sb}}{\hat{s}^2} \right) \left(1 - \frac{2\hat{s}m_{\widetilde{s}\widetilde{b}_1}^2}{\hat{u}_{sb}\hat{t}_{sb}} + \frac{2\hat{s}^2m_{\widetilde{s}\widetilde{b}_1}^4}{\hat{u}_{sb}^2\hat{t}_{sb}^2} \right). \quad (12) \end{aligned}$$

The integrated cross section is given by

$$\begin{aligned} \sigma(gg \rightarrow \widetilde{s}\widetilde{b}_1\widetilde{s}\widetilde{b}_1^*) &= \frac{\pi\alpha_s^2}{\hat{s}} \left[\beta_{sb} \frac{5\hat{s} + 62m_{\widetilde{s}\widetilde{b}_1}^2}{48\hat{s}} \right. \\ & \left. + \frac{m_{\widetilde{s}\widetilde{b}_1}^2}{6\hat{s}} \frac{m_{\widetilde{s}\widetilde{b}_1}^2 + 4\hat{s}}{\hat{s}} \ln \frac{1 - \beta_{sb}}{1 + \beta_{sb}} \right]. \quad (13) \end{aligned}$$

For completeness we also give the expressions for $s\bar{s}, b\bar{b} \rightarrow \widetilde{s}\widetilde{b}_1\widetilde{s}\widetilde{b}_1^*$ cross sections,

$$\begin{aligned} & \frac{d\sigma}{d\cos\theta^*}(s\bar{s} \rightarrow \widetilde{s}\widetilde{b}_1\widetilde{s}\widetilde{b}_1^*) \\ &= \frac{2\pi\alpha_s^2\beta_{sb}}{9\hat{s}} \left(\frac{1}{4}(1 - \beta_{sb}^2 \cos^2\theta^*) - \frac{m_{\widetilde{s}\widetilde{b}_1}^2}{\hat{s}} \right) \\ & \times \left[1 - \frac{1}{3} \frac{\hat{s}}{\hat{t}_{\widetilde{g}}} \cos^2\theta_m + \frac{1}{2} \frac{\hat{s}^2}{\hat{t}_{\widetilde{g}}^2} \cos^4\theta_m \right]. \quad (14) \end{aligned}$$

Integrating over $\cos\theta^*$ gives

$$\begin{aligned} \sigma(s\bar{s} \rightarrow \widetilde{s}\widetilde{b}_1\widetilde{s}\widetilde{b}_1^*) &= \frac{2\pi\alpha_s^2}{27\hat{s}^3} \left\{ \beta_{sb}\hat{s}(\hat{s}\beta_{sb}^2 - 6\hat{s}\cos^4\theta_m \right. \\ & \left. + \cos^2\theta_m(\hat{s} + 2m_{\widetilde{g}}^2)) + \cos^2\theta_m(2m_{\widetilde{g}}^4 - 3\hat{s}\cos^2\theta_m \right. \\ & \left. \times (\hat{s} + 2m_{\widetilde{g}}^2) + 2\hat{s}m_{\widetilde{g}}^2 \right\} \log \left(\frac{\hat{s} + 2m_{\widetilde{g}}^2 - \beta_{sb}\hat{s}}{\hat{s} + 2m_{\widetilde{g}}^2 + \beta_{sb}\hat{s}} \right), \quad (15) \end{aligned}$$

where $m_{\widetilde{g}}^2 = m_g^2 - m_{\widetilde{s}\widetilde{b}_1}^2$. The cross section for $b\bar{b} \rightarrow \widetilde{s}\widetilde{b}_1\widetilde{s}\widetilde{b}_1^*$ can be obtained by replacing $\cos^2\theta_m \leftrightarrow \sin^2\theta_m$ in Eqs. (14) and (15). On the other hand, the processes $s\bar{b}, \overline{s}\widetilde{b} \rightarrow \widetilde{s}\widetilde{b}_1\widetilde{s}\widetilde{b}_1^*$ only have the t -channel gluino exchange diagram, and its differential cross section is given by

$$\begin{aligned} & \frac{d\sigma}{d\cos\theta^*}(s\bar{b} \rightarrow \widetilde{s}\widetilde{b}_1\widetilde{s}\widetilde{b}_1^*) = \frac{\pi\alpha_s^2\beta_{sb}}{9} \frac{\hat{s}}{\hat{t}_{\widetilde{g}}^2} \cos^2\theta_m \sin^2\theta_m \\ & \times \left(\frac{1}{4}(1 - \beta_{sb}^2 \cos^2\theta^*) - \frac{m_{\widetilde{s}\widetilde{b}_1}^2}{\hat{s}} \right). \quad (16) \end{aligned}$$

Direct production of $\widetilde{s}\widetilde{b}_1\widetilde{s}\widetilde{b}_1$

Production of $\widetilde{s}\widetilde{b}_1\widetilde{s}\widetilde{b}_1$ ($\widetilde{s}\widetilde{b}_1^*\widetilde{s}\widetilde{b}_1^*$) pair requires ss , sb or bb ($\overline{s}\overline{s}$, $\overline{s}\overline{b}$, or $\overline{b}\overline{b}$) in the initial state. The process proceeds via t - and u -channel gluino-exchange diagrams, as shown in Fig. 2(d). The differential cross section is given by

$$\begin{aligned} \frac{d\sigma}{d\cos\theta^*}(ss\rightarrow\widetilde{s}\widetilde{b}_1\widetilde{s}\widetilde{b}_1) &= \frac{\pi\alpha_s^2\beta_{sb}}{18}\cos^4\theta_m m_g^2 \left[\frac{1}{\hat{t}_g^2} + \frac{1}{\hat{u}_g^2} - \frac{2}{3} \frac{1}{\hat{t}_g} \frac{1}{\hat{u}_g} \right], \\ & \quad (17) \end{aligned}$$

where we have explicitly put in the factor 1/2 and so $\cos\theta^*$ ranges from -1 to 1 . Integrating over the angle the total cross section is

$$\begin{aligned} \sigma(ss\rightarrow\widetilde{s}\widetilde{b}_1\widetilde{s}\widetilde{b}_1) &= \frac{\pi\alpha_s^2\beta_{sb}}{18}\cos^4\theta_m m_g^2 \left[\frac{4}{m_-^4 + \hat{s}m_g^2} \right. \\ & \quad \left. + \frac{8}{3\beta_{sb}\hat{s}} \frac{1}{\hat{s} + 2m_-^2} \log\left(\frac{\hat{s} + 2m_-^2 - \beta_{sb}\hat{s}}{\hat{s} + 2m_-^2 + \beta_{sb}\hat{s}}\right) \right]. \\ & \quad (18) \end{aligned}$$

The cross section for $bb\rightarrow\widetilde{s}\widetilde{b}_1\widetilde{s}\widetilde{b}_1$ can be obtained by replacing $\cos^4\theta_m\leftrightarrow\sin^4\theta_m$, while that for $sb\rightarrow\widetilde{s}\widetilde{b}_1\widetilde{s}\widetilde{b}_1$ by replacing $\cos^4\theta_m\leftrightarrow\cos^2\theta_m\sin^2\theta_m$. Note that, for example, the amplitude of $bb\rightarrow\widetilde{s}\widetilde{b}_1\widetilde{s}\widetilde{b}_1$ contains the phase factor $e^{-2i\sigma}$. Obviously, when we calculate the cross section the phase factor drops out.

Feed down from gluino-pair production

We employ a tree-level calculation for gluino-pair production, though including the next-to-leading order (NLO) corrections [9] the cross section may increase by more than 50%. However, the overall gluino-pair production is small because we have chosen the gluino mass to be at least 500 GeV. Whether we include the NLO correction or not does not affect our conclusion.

Here we give the tree-level formulas for gluino-pair production, without the squark in the t - and u -channels,

$$\begin{aligned} \frac{d\sigma}{d\cos\theta^*}(q\bar{q}\rightarrow\widetilde{g}\widetilde{g}) &= \frac{2\pi\alpha_s^2}{3\hat{s}}\beta_g \frac{\hat{t}_g^2 + \hat{u}_g^2 + 2m_g^2\hat{s}}{\hat{s}^2}, \\ \frac{d\sigma}{d\cos\theta^*}(gg\rightarrow\widetilde{g}\widetilde{g}) &= \frac{9\pi\alpha_s^2}{16\hat{s}}\beta_g \left(1 - \frac{\hat{t}_g\hat{u}_g}{\hat{s}^2} \right) \left(\frac{\hat{s}^2}{\hat{t}_g\hat{u}_g} \right. \\ & \quad \left. - 2 + \frac{4m_g^2\hat{s}}{\hat{t}_g\hat{u}_g} - \frac{4\hat{s}^2 m_g^4}{\hat{t}_g^2\hat{u}_g^2} \right), \quad (19) \end{aligned}$$

where we have put in the factor of 1/2 for identical particles in the final state, and $\cos\theta^*$ is from -1 to 1 . The integrated cross sections are given by

$$\begin{aligned} \sigma(q\bar{q}\rightarrow\widetilde{g}\widetilde{g}) &= \frac{8\pi\alpha_s^2}{9\hat{s}}\beta_g \left(1 + \frac{2m_g^2}{\hat{s}} \right), \\ \sigma(gg\rightarrow\widetilde{g}\widetilde{g}) &= \frac{3\pi\alpha_s^2}{4\hat{s}} \left[-\beta_g \left(4 + 17\frac{m_g^2}{\hat{s}} \right) \right. \\ & \quad \left. + 3 \left(\frac{4m_g^4}{\hat{s}^2} - \frac{4m_g^2}{\hat{s}} - 1 \right) \log\left(\frac{1-\beta_g}{1+\beta_g}\right) \right]. \quad (20) \end{aligned}$$

For completeness we also give the cross sections for $s\bar{s}\rightarrow\widetilde{g}\widetilde{g}$,

$$\begin{aligned} \frac{d\sigma}{d\cos\theta^*}(s\bar{s}\rightarrow\widetilde{g}\widetilde{g}) &= \frac{2\pi\alpha_s^2}{3\hat{s}}\beta_g \left\{ \frac{\hat{t}_g^2 + \hat{u}_g^2 + 2m_g^2\hat{s}}{\hat{s}^2} \right. \\ & \quad \left. + \frac{2}{9}\cos^4\theta_m \left(\frac{\hat{t}_g^2}{\hat{t}_{sb}} + \frac{\hat{u}_g^2}{\hat{u}_{sb}} \right) \right. \\ & \quad \left. + \frac{1}{2}\cos^2\theta_m \frac{1}{\hat{s}} \left(\frac{\hat{s}m_g^2 + \hat{t}_g^2}{\hat{t}_{sb}} + \frac{\hat{s}m_g^2 + \hat{u}_g^2}{\hat{u}_{sb}} \right) \right. \\ & \quad \left. + \frac{1}{18}\cos^4\theta_m \frac{\hat{s}m_g^2}{\hat{u}_{sb}\hat{t}_{sb}} \right\}. \quad (21) \end{aligned}$$

The formulas for $b\bar{b}\rightarrow\widetilde{g}\widetilde{g}$ can be obtained by replacing $\cos\theta_m$ by $\sin\theta_m$. Note that $s\bar{b},\overline{s}b\rightarrow\widetilde{g}\widetilde{g}$ only occur via the t - and u -channel diagrams, and the differential cross section is given by

$$\begin{aligned} \frac{d\sigma}{d\cos\theta^*}(s\bar{b}\rightarrow\widetilde{g}\widetilde{g}) &= \frac{\pi\alpha_s^2}{27\hat{s}}\beta_g \cos^2\theta_m \sin^2\theta_m \left\{ 4 \left(\frac{\hat{t}_g^2}{\hat{t}_{sb}^2} + \frac{\hat{u}_g^2}{\hat{u}_{sb}^2} \right) \right. \\ & \quad \left. + \frac{\hat{s}m_g^2}{\hat{u}_{sb}\hat{t}_{sb}} \right\}. \quad (22) \end{aligned}$$

We have chosen the mass of gluino to be at least 500 GeV, in order not to upset lower energy constraints such as $b\rightarrow s\gamma$ rate, and not to violate the bound from direct search at the Tevatron [8]. The gluino so produced will decay into a strange or beauty quark plus the strange-beauty squark $\widetilde{s}\widetilde{b}_1$. Therefore, gluino-pair production gives two more jets in the final state than direct production. Having more jet activities to tag on may help the detection, especially when b -tagging is employed. We shall discuss in more detail in the next section when we treat the decay of the $\widetilde{s}\widetilde{b}_1$. Nevertheless, since the gluino mass is above 500 GeV, the production rate at the Tevatron is rather small. For a gluino mass of 500 GeV, the production cross section is 2.9 fb, which may increase to about 4 fb after taking into account NLO correction [9]. However, it helps only a little as far as the strange-

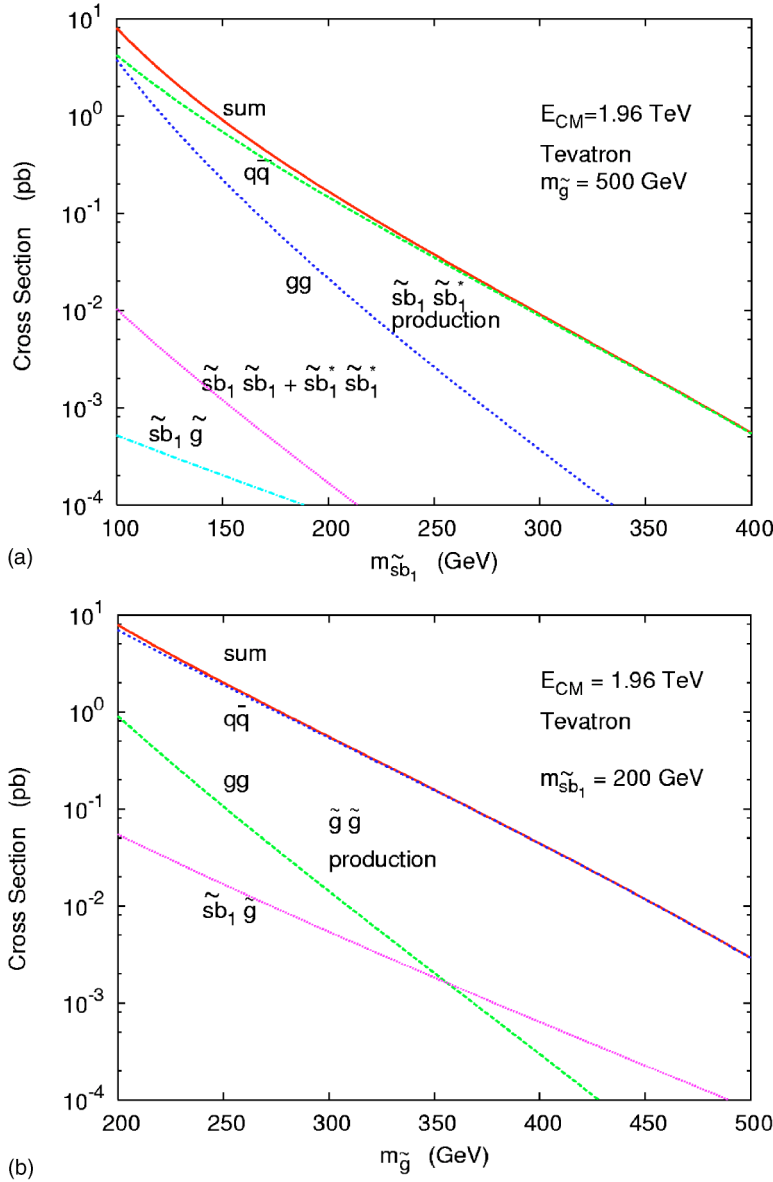


FIG. 3. Total cross section for direct production of (a) the $\tilde{s}\tilde{b}_1\tilde{s}\tilde{b}_1^*$ pair and (b) the $\tilde{g}\tilde{g}$ pair at the Tevatron. The individual gg fusion and $q\bar{q}$ annihilation contributions are shown. In (a) we also show $\tilde{s}\tilde{b}_1\tilde{s}\tilde{b}_1 + \tilde{s}\tilde{b}_1^*\tilde{s}\tilde{b}_1^*$ production, and $\tilde{s}\tilde{b}_1\tilde{g} + \tilde{s}\tilde{b}_1^*\tilde{g}$ production, where we have fixed $m_{\tilde{g}} = 500$ GeV. In (b) we also show $\tilde{s}\tilde{b}_1\tilde{g} + \tilde{s}\tilde{b}_1^*\tilde{g}$ production, where we have fixed $m_{\tilde{s}\tilde{b}_1} = 200$ GeV.

beauty squark pair production is concerned, unless the squark mass is above 300 GeV. We will take this into account in our analysis.

Production of $\tilde{s}\tilde{b}_1\tilde{g}$

There is another process $s(b)g \rightarrow \tilde{g}\tilde{s}\tilde{b}_1$ that can contribute to strange-beauty squark production, but it requires either s or b in the initial state. The differential cross section for the process is given by

$$\frac{d\sigma}{d\cos\theta^*}(sg \rightarrow \tilde{s}\tilde{b}_1\tilde{g}) = \frac{\pi\alpha_s^2}{192\hat{s}}\beta_{sbg}\cos^2\theta_m \left[24 \left(1 - \frac{2\hat{s}\hat{u}_{sb}}{\hat{t}_g^2} \right) - \frac{8}{3} \right] \left[-\frac{\hat{t}_g^-}{\hat{s}} + \frac{2(m_g^2 - m_{\tilde{s}\tilde{b}_1}^2)\hat{t}_g^-}{\hat{s}\hat{u}_{sb}} \left(1 + \frac{m_{\tilde{s}\tilde{b}_1}^2}{\hat{u}_{sb}} + \frac{m_g^2}{\hat{t}_g^-} \right) \right]. \quad (23)$$

For the bg initial state, the above formula is modified by changing $\cos^2\theta_m \leftrightarrow \sin^2\theta_m$.

B. Production cross sections

Folding in parton distributions with the parton level cross sections, the cross sections for direct $\tilde{s}\tilde{b}_1\tilde{s}\tilde{b}_1^*$ pair production at the Tevatron are shown in Fig. 3(a), where we give the individual gg and $q\bar{q}$ contributions. As expected, the gluon fusion contribution is subdominant for $m_{\tilde{s}\tilde{b}_1} \gtrsim 100$ GeV. We also show in Fig. 3(a) the same sign $\tilde{s}\tilde{b}_1\tilde{s}\tilde{b}_1 + \tilde{s}\tilde{b}_1^*\tilde{s}\tilde{b}_1^*$ production, and the associated $\tilde{s}\tilde{b}_1\tilde{g} + \tilde{s}\tilde{b}_1^*\tilde{g}$ production. These processes are three orders of magnitude smaller than $\tilde{s}\tilde{b}_1\tilde{s}\tilde{b}_1^*$ pair production, and can be safely ignored at the Tevatron.

Glino-pair production cross sections at the Tevatron are given in Fig. 3(b). Similar to squark-pair production, gluino-pair production is dominated by $q\bar{q}$ pair annihilation. For a

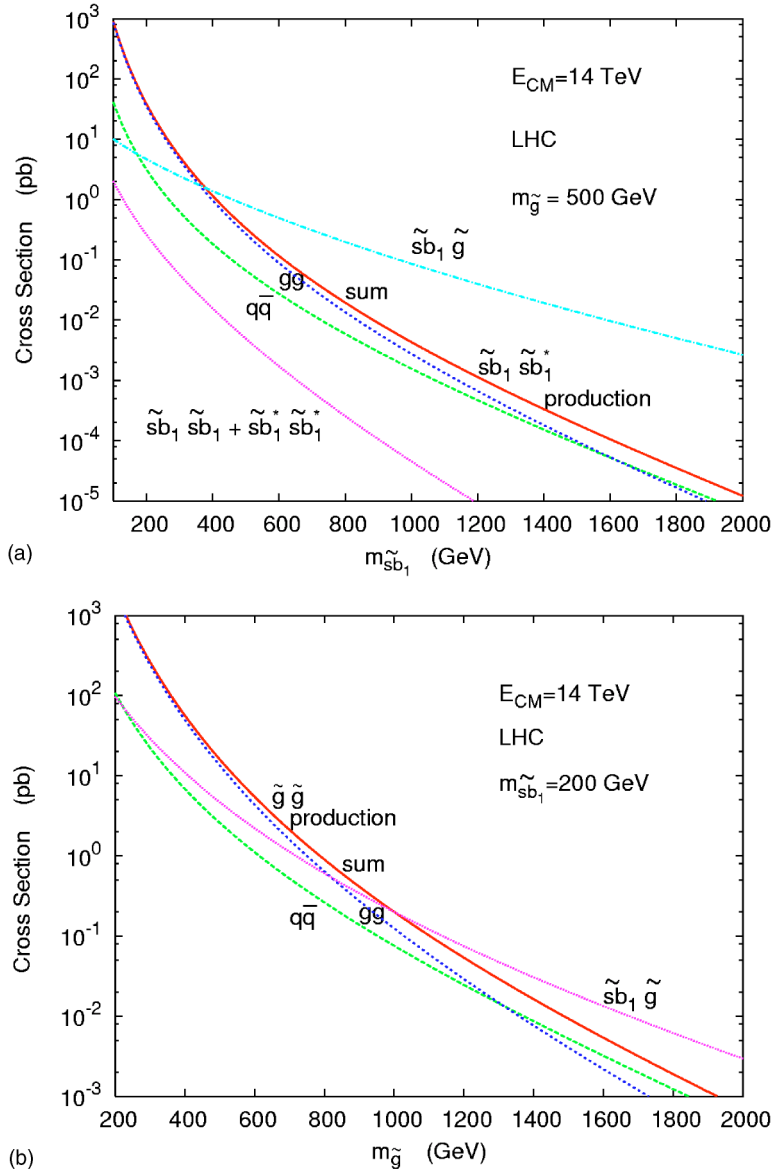


FIG. 4. Total cross section for direct production of (a) the $\tilde{s}b_1\tilde{s}b_1^*$ pair and (b) the $\tilde{g}\tilde{g}$ pair at the LHC. The individual $g\bar{g}$ fusion and $q\bar{q}$ annihilation contributions are shown. In (a) we also show $\tilde{s}b_1\tilde{s}b_1 + \tilde{s}b_1^*\tilde{s}b_1^*$ production, and $\tilde{s}b_1\tilde{g} + \tilde{s}b_1^*\tilde{g}$ production, where we have fixed $m_{\tilde{g}} = 500$ GeV. In (b) we also show $\tilde{s}b_1\tilde{g} + \tilde{s}b_1^*\tilde{g}$ production, where we have fixed $m_{\tilde{s}b_1} = 200$ GeV.

gluino mass of 500 GeV the cross section is only a few fb, and thus this contribution becomes comparable to direct $\tilde{s}b_1$ pair production only when $m_{\tilde{s}b_1} \gtrsim 300$ GeV. Therefore, at low $m_{\tilde{s}b_1}$ the gluino contribution is very small, while at high $m_{\tilde{s}b_1}$ the gluino contribution can extend the sensitivity further.

The situation is different at the LHC. We show the corresponding results in Figs. 4(a) and 4(b), respectively. We see that gluon fusion now dominates over $q\bar{q}$ pair annihilation. Furthermore, gluino pair production and squark pair production cross sections are both above 10 pb for $m_{\tilde{s}b_1} = 200$ GeV and $m_{\tilde{g}} = 500$ GeV, and both contributions have to be taken into account at the LHC. We also show the associated $\tilde{s}b_1\tilde{g} + \tilde{s}b_1^*\tilde{g}$ production cross section in Figs. 4(a) and 4(b). These curves are somewhat misleading, however, that their cross sections become larger than $\tilde{s}b_1$ -pair (or gluino-pair) production for large enough $m_{\tilde{s}b_1}$ ($m_{\tilde{g}}$). This is simply because the mass of $m_{\tilde{g}}$ is held fixed at 500 GeV in Fig. 4(a)

while $m_{\tilde{s}b_1}$ is fixed at 200 GeV in Fig. 4(b). Therefore, for very large mass the $\tilde{s}b_1$ - or \tilde{g} -pair production become suppressed.

Before we discuss detection, we need to understand how the $\tilde{s}b_1$ squark decays, to which we now turn.

IV. DECAY AND DETECTION OF THE STRANGE-BEAUTY SQUARK

If the SUSY scale is set at TeV, all SUSY particles should be around this scale, unless one has cancellation mechanisms in the diagonalization of the neutralino, chargino, or sfermion mass matrices that allow some of them to become close to the electroweak scale. The lightness of the $\tilde{s}b_1$ in our scenario is a particular example of this type. This in fact involves fine-tuning. However, the fine-tuning is comparable [3] to what is already seen in the quark mixing matrix. In any case, we do not discuss it further here.

We concentrate on squark-pair production at the Tevatron. We put the LHC study aside as its discussion is more intricate, but of less immediate interest. It is clear from Fig. 3(a) that the dominant production channels are $gg, qq \rightarrow \widetilde{s}\widetilde{b}_1\widetilde{s}\widetilde{b}_1^*$. Gluino-pair production with $m_{\widetilde{g}} = 500$ GeV, followed by gluino decay, is only relevant for $m_{\widetilde{s}\widetilde{b}_1} \gtrsim 300$ GeV. On the other hand, $\widetilde{s}\widetilde{b}_1\widetilde{s}\widetilde{b}_1$ and $\widetilde{s}\widetilde{b}_1^*\widetilde{s}\widetilde{b}_1^*$ pair production and the associated production can be safely ignored.

In the following, we take on three situations for the decay of the strange-beauty squark:

(i) When the $\widetilde{s}\widetilde{b}_1$ is the lightest supersymmetric particle (LSP) and R -parity is conserved.¹ This stable $\widetilde{s}\widetilde{b}_1$ case also includes the case when the $\widetilde{s}\widetilde{b}_1$ is stable within the detector but decays outside.

(ii) The $\widetilde{s}\widetilde{b}_1$ is the LSP but R -parity is violated such that it will decay into 2 jets or 1 lepton plus 1 jet.

(iii) The $\widetilde{s}\widetilde{b}_1$ is the next-to-lightest supersymmetric particle (NLSP), and either neutralino (in supergravity) or gravitino (gauge-mediated) is the LSP such that $\widetilde{s}\widetilde{b}_1$ will decay into a strange or beauty quark plus the neutralino or gravitino.

Among the three cases we particularly emphasize case (iii), which is the most popular. In the SUGRA models, one has $\widetilde{s}\widetilde{b}_1 \rightarrow s/b\widetilde{\chi}_1^0$, while in gauge-mediated models $\widetilde{s}\widetilde{b}_1 \rightarrow s/b\widetilde{G}$ or $\widetilde{s}\widetilde{b}_1 \rightarrow s/b\widetilde{\chi}_1^0 \rightarrow s/b\gamma\widetilde{G}$. In any case, there will be b/s -quark jets plus a large missing energy in the final state. We simplify the picture by modelling the decay as $\widetilde{s}\widetilde{b}_1 \rightarrow s/b\widetilde{\chi}_1^0$ and by varying the mass of the neutralino.

A. Stable strange-beauty squark

In this case, the $\widetilde{s}\widetilde{b}_1\widetilde{s}\widetilde{b}_1^*$ pair so produced will hadronize into color-neutral hadrons by combining with some light quarks. Such objects are strongly-interacting massive particles, electrically either neutral or charged. If the hadron is electrically neutral, it will pass through the tracker with little trace. The interactions in the calorimetry would be rather intricate, since charge exchange (\bar{d} replaced by \bar{u} when

passing by a nucleus) can readily occur.² However, the hadron could be electrically charged with equal probability. In this case, the hadron will undergo ionization energy loss in the central tracking system, hence behaves like a ‘‘heavy muon.’’ Let us discuss this possibility since it is more straightforward.

The energy loss dE/dx due to ionization in the detector material is very standard [10]. Essentially, the penetrating particle loses energy by exciting the electrons of the material. Ionization energy loss dE/dx is a function of $\beta\gamma \equiv p/M$ and the charge Q of the penetrating particle. The dependence on the mass M of the penetrating particle comes in through $\beta\gamma$ for a large mass M and small γ [10]. In other words, dE/dx is the same for different masses if the $\beta\gamma$ values of these particles are the same. For the range of $\beta\gamma$ between 0.1 and 1 that we are interested in, dE/dx has almost no explicit dependence on the mass M of the penetrating particle. Therefore, when dE/dx is measured in an experiment, the $\beta\gamma$ can be deduced, which then gives the mass of the particle if the momentum p is also measured. Hence, dE/dx is a good tool for particle identification for massive stable charged particles. In fact, the CDF Collaboration has made a few searches for massive stable charged particles [11]. The CDF analyses required that the particle produces a track in the central tracking chamber and/or the silicon vertex detector, and at the same time penetrates to the outer muon chamber.³

The CDF detector has a silicon vertex detector and a central tracking chamber (which has a slightly better resolution in this regard), which can measure the energy loss (dE/dx) of a particle via ionization, especially at low $\beta\gamma < 0.85$ ($\beta < 0.65$) where $dE/dx \sim 1/\beta^2$. Once the dE/dx is measured, the mass M of the particle can be determined if the momentum p is measured simultaneously. Furthermore, the particle is required to penetrate through the detector material and make it to the outer muon chamber, provided that it has an initial $\beta > 0.25 - 0.45$ depending on the mass of the particle [11]. Therefore, the CDF requirement on β or $\beta\gamma$ is (note $\beta\gamma = \beta/\sqrt{1-\beta^2}$)

$$0.25 - 0.45 \leq \beta < 0.65 \quad \Leftrightarrow \quad 0.26 - 0.50 \leq \beta\gamma < 0.86.$$

The lower limit is to make sure that the penetrating particle can make it to the outer muon chamber, while the upper limit makes sure that the ionization loss in the tracking chamber is sufficient for detection. CDF has searched for such massive stable charged particles, but did not find any. The limits placed on the mass of these particles are model dependent [12]. Some theoretical studies on massive stable charged par-

¹A concern of this squark-LSP scenario is that the dark matter cannot be a colored or charged particle. However, one has to actually calculate the relic density of the LSP. Since the squarks annihilate into SM particles via strong interaction, the relic density, which scales inversely with the annihilation cross section, is in fact very small, as long as the squark mass is less than 1–2 TeV. Therefore, such a squark-LSP scenario is safe and consistent with cosmological constraints. A similar study on gluino-LSP scenario was performed in Ref. [13]. In these cases, the dark matter has to be some other particle or substance, which might be viewed as a drawback of such pictures, but in principle they are possible.

²An issue arises when the neutral hadron containing the $\widetilde{s}\widetilde{b}_1$ may ‘‘bounce’’ into a charged hadron when the internal \bar{d} is knocked off and replaced by a \bar{u} , for example. The probability of such a scattering depends crucially on the mass spectrum of the hadrons formed by $\widetilde{s}\widetilde{b}_1$. In reality, we know very little about the spectrum, so we simply assume a 50% chance that a $\widetilde{s}\widetilde{b}_1$ will hadronize into a neutral or charged hadron.

³In run II, the requirement to reach the outer muon chamber may be dropped but it leads to a lower signal-to-background ratio.

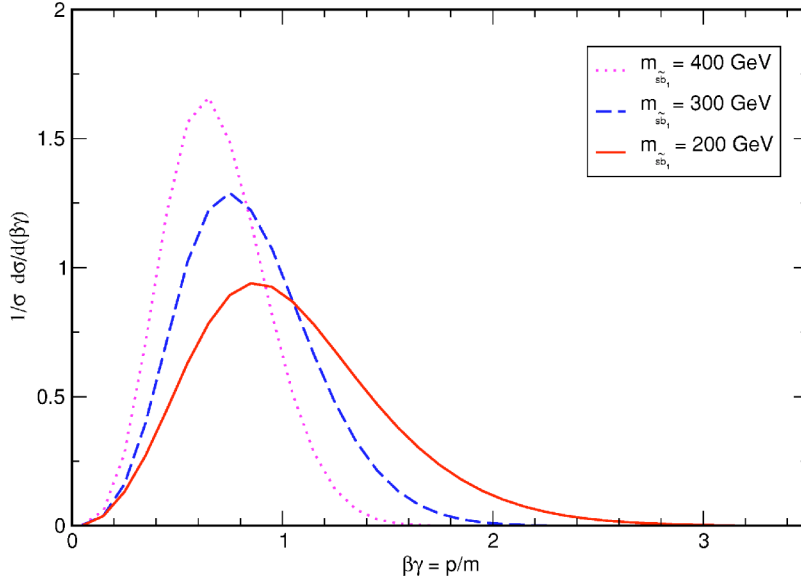


FIG. 5. The $\beta\gamma \equiv p/m_{\tilde{s}b_1}$ spectrum for squark-pair production at the Tevatron, where p is the squark momentum.

ticles exist for gluino LSP models [13], colored Higgs bosons and Higgsinos [14], and scalar leptons [15].

We use a similar analysis for strange-beauty squark pair production with the squark remaining stable within the detector. We employ the following acceptance cuts on the squarks

$$p_T(\tilde{s}b_1) > 20 \text{ GeV}, \quad |y(\tilde{s}b_1)| < 2.0, \quad 0.25 < \beta\gamma < 0.85. \quad (24)$$

In Fig. 5, we show the $\beta\gamma$ distribution for direct $\tilde{s}b_1$ pair production at the Tevatron. It is clear that more than half of the cross sections satisfy the $\beta\gamma$ cut. This is easy to understand as the squark is massive such that they are produced close to threshold. In Table I we show the cross sections from direct $\tilde{s}b_1$ pair production with all the acceptance cuts in Eq. (24), for detecting 1 massive stable charged particle (MCP), 2 MCPs, or at least 1 MCPs in the final state. The latter cross section is the simple sum of the former two. We have used a probability of 50% that the $\tilde{s}b_1$ will hadronize into a charged hadron. In the table, we also give the feed down from gluino-pair production in the parentheses. It is

TABLE I. Cross sections for direct strange-beauty squark pair production at the Tevatron, with the cuts of Eq. (24). Here $\sigma_{1\text{MCP}}$, $\sigma_{2\text{MCP}}$ denote requiring the detection of 1, 2 massive stable charged particles (MCP) in the final state, respectively. Requiring at least one MCP in the final state corresponds to simply adding the two cross sections. In parentheses, we give the contribution fed down from direct gluino-pair production.

$m_{\tilde{s}b_1}$ (GeV)	$\sigma_{1\text{MCP}}$ (fb)	$\sigma_{2\text{MCP}}$ (fb)	$\sigma_{\geq 1\text{MCP}}$ (fb)
200	41 (0.46)	9.3 (0.02)	50 (0.48)
250	10.9 (0.96)	2.8 (0.14)	14 (1.1)
300	3.1 (1.2)	0.91 (0.3)	4.0 (1.5)
350	0.87 (1.3)	0.29 (0.43)	1.2 (1.8)
400	0.23 (1.4)	0.088 (0.48)	0.32 (1.8)
450	0.058 (1.4)	0.024 (0.51)	0.082 (1.9)

obvious that the feed down is relatively small for $m_{\tilde{s}b_1} \lesssim 300$ GeV, but becomes significant for $m_{\tilde{s}b_1} \gtrsim 300$ GeV. Requiring about 10 such events as suggestive evidence, the sensitivity can reach up to almost $m_{\tilde{s}b_1} \approx 300$ GeV with an integrated luminosity of 2 fb^{-1} .

B. $\tilde{s}b_1$ as LSP but R -parity is violated

In this case the $\tilde{s}b_1$ pair so produced will decay via the R -parity violating terms $\lambda' L Q D^c$ or $\lambda'' U^c D^c D^c$ in the superpotential. In general, λ' and λ'' couplings are not considered simultaneously, otherwise it will lead to unwanted baryon decay. Since nonzero λ'' couplings would give only multi-jets in the final state, which would likely be buried under QCD backgrounds, we only consider the λ' coupling in the following.

By the right-handed nature of the strange-beauty squark in our scenario, the third index in the λ' coupling is either 2 or 3, and we only consider λ'_{i13} , λ'_{i12} with $i=1, 2$. The strange-beauty squark will decay into $e^- u$ or $\mu^- c$. Therefore, the strange-beauty squark behaves like scalar leptoquarks of the first or second generation, respectively. The decay mode of $\tau^- t$ is not feasible at the Tevatron. The current published limits [16] from CDF are 213 GeV and 202 GeV for the first and second generation leptoquarks while $D\bar{D}$ obtained limits of 225 and 200 GeV, respectively. The latest preliminary limits [16] from CDF are 230 and 240 GeV, respectively, while those from $D\bar{D}$ are 231 and 186 GeV, respectively. In one of the preliminary plots, the combined limits from all CDF and $D\bar{D}$ run I and II data can push the first generation leptoquark limit to around 260 GeV, which is very impressive.⁴ The sensitivity reach in run II has been studied

⁴These limits are for the leptoquarks that decay entirely into charged leptons and quarks. If the leptoquark also decays into a neutrino and a quark, the corresponding limit is somewhat weaker.

TABLE II. Cross sections in fb for direct squark-pair production at the Tevatron with $\sqrt{s}=1.96$ TeV, for 0, 1, 2 b -tagged events. The imposed cuts are $p_{Tj}>15$ GeV, $|\eta_j|<2$, and $\not{p}_T>40$ GeV, b -tagging efficiency $\epsilon_{btag}=0.6$, and a mistag probability of $\epsilon_{mis}=0.0$. In parentheses, we give the contribution fed down from direct gluino-pair production.

$m_{\tilde{s}b_1}$ (GeV)	0 b -tag	1 b -tag	2 b -tag	0 b -tag	1 b -tag	2 b -tag
		$\sin^2\theta_m=1$			$\sin^2\theta_m=0.75$	
150	115 (0.11)	288 (0.54)	175 (2.2)	190 (0.29)	284 (0.89)	104 (1.6)
200	26 (0.091)	70 (0.49)	47 (2.2)	44 (0.27)	70 (0.85)	28 (1.7)
250	6.1 (0.090)	17 (0.49)	11 (2.2)	11 (0.27)	17 (0.85)	6.8 (1.7)
300	1.5 (0.090)	4.2 (0.49)	2.9 (2.2)	2.6 (0.27)	4.2 (0.85)	1.7 (1.7)
350	0.38(0.090)	1.1 (0.49)	0.72(2.2)	0.66 (0.27)	1.1 (0.86)	0.43 (1.7)
400	0.094(0.090)	0.26(0.49)	0.18 (2.2)	0.16 (0.27)	0.26 (0.86)	0.11 (1.7)
450	0.022(0.096)	0.06(0.51)	0.04 (2.2)	0.038 (0.28)	0.061 (0.87)	0.025 (1.7)
		$\sin^2\theta_m=0.5$			$\sin^2\theta_m=0.25$	
150	283 (0.66)	243 (1.2)	51 (1.0)	395 (1.3)	165 (1.1)	17 (0.40)
200	68 (0.63)	61 (1.1)	14 (1.0)	96 (1.3)	42 (1.1)	4.6 (0.42)
250	16 (0.62)	15 (1.1)	3.3 (1.0)	23 (1.3)	10 (1.1)	1.1 (0.42)
300	4.0 (0.63)	3.7 (1.1)	0.84 (1.0)	5.8 (1.3)	2.5 (1.1)	0.28 (0.42)
350	1.0 (0.63)	0.93 (1.1)	0.21 (1.0)	1.4 (1.3)	0.64 (1.1)	0.071 (0.43)
400	0.25 (0.63)	0.23 (1.2)	0.052 (1.1)	0.35 (1.3)	0.16 (1.1)	0.017 (0.43)
450	0.058 (0.64)	0.053 (1.2)	0.012 (1.0)	0.083 (1.3)	0.037 (1.1)	0.004 (0.42)

in TeV2000 report [17]. The reach on the first or second generation leptoquarks are 235 and 325 GeV with a luminosity of 1 and 10 fb^{-1} , respectively. Apparently, the preliminary limits obtained by CDF and DØ with a luminosity of $\sim 200 \text{pb}^{-1}$ are already very close to or even surpass the sensitivity reach quoted in TeV2000 report. Therefore, we believe that the limit that can be reached at the end of run II (2 fb^{-1}) is very likely above 300 GeV. With an order more luminosity, the limit may be able to reach 350 GeV: see the total cross section in Fig. 3(a).

C. $\tilde{s}b_1$ is the NLSP

In this case the $\tilde{s}b_1$ so produced will decay into a strange or beauty quark plus the neutralino in the supergravity framework or the gravitino (or via an intermediate neutralino into a photon and a gravitino) in the gauge-mediated framework. Experimentally, the signature is similar, except for the fact that the neutralino is of order 100 GeV while the gravitino is virtually massless compared to the collider energy. We simplify the picture by modelling the decay as $\tilde{s}b_1 \rightarrow s/b\tilde{\chi}_1^0$ and by varying the mass of the neutralino. In addition, we have to check if the strange-beauty squark will decay *within* the detector. In the SUGRA case, the decay rate is of electroweak strength hence the decay is prompt. However, in the gauge-mediated case, the decay rate scales as $\sim 1/F_{\text{SUSY}}^2$, where $\sqrt{F_{\text{SUSY}}}$ is the dynamical SUSY breaking scale. Therefore, if $\sqrt{F_{\text{SUSY}}}$ is so large, the strange-beauty squark behaves like a *stable* particle inside the detector. Reference [15] showed that, for $\sqrt{F_{\text{SUSY}}}\gtrsim 10^7$ GeV the scalar tau NLSP would behave like a stable particle inside a typical particle detector. This value applies to the strange-beauty squark as well, up to a color factor. If it is stable, one goes

back to case (i). So here we focus on the prompt decay of the strange-beauty squark, which is considered to be the more popular case.

There are 2 quark jets in the final state of $\tilde{s}b_1\tilde{s}b_1^*$ pair production, each of them either strange or beauty flavored, and with large missing energy due to the neutralinos or gravitinos. We impose the following cuts on the jets and missing transverse momentum, and we choose the following b -tagging and mistag efficiencies⁵

$$p_{Tj}>15 \text{ GeV}, \quad |\eta_j|<2.0, \quad \not{p}_T>40 \text{ GeV},$$

$$\epsilon_{btag}=0.6, \quad \epsilon_{mis}=0.05.$$

Note that the branching ratio of the strange-beauty squark into a b quark scales as $\sin^2\theta_m$.

We have tested our parton-level Monte Carlo program as follows. Most events generated pass the jet (p_{Tj} and $|\eta_j|$) requirements, as long as the mass difference between the $\tilde{s}b_1$ and $\tilde{\chi}_1^0$ is larger than 50 GeV. Taking $B(\tilde{s}b_1 \rightarrow b\tilde{\chi}_1^0)=1$ (a standard \tilde{b} squark), we verify our input b -tagging efficiency, i.e. the ratio of 0:1:2 b -tagged jets is 16:48:36. Choosing the $B(\tilde{s}b_1 \rightarrow b\tilde{\chi}_1^0)=0.5$ value expected in our scenario, the ratio of 0:1:2 b -tagged jets becomes 49:42:9. The double-tag approach becomes far less effective, but if we only require at least one b -tagged jet in the final state, the overall efficiency is about 0.5. On one hand, this is a dilution compared to the standard \tilde{b} squark pair production, which gives overall efficiency of 0.84. On the other hand, the prospect is still very good for run II.

⁵The mistag efficiency is the probability that a non- b jet is detected as a b -jet.

In Table II, we show the cross sections in units of fb for direct squark-pair production, with the squark decaying into either s/b plus a neutralino at the Tevatron with $\sqrt{s} = 1.96$ TeV. We have set $m_{\tilde{\chi}_1^0} = 100$ GeV; other values of $m_{\tilde{\chi}_1^0}$ do not affect the result in any significant way, so long as the mass difference between the squark and neutralino is larger than about 50 GeV. Note that the production cross section itself is almost independent of $\sin^2\theta_m$ and $m_{\tilde{g}}$. This is because the dominant production channel is the standard QCD s -channel $q\bar{q} \rightarrow \tilde{s}\tilde{b}_1\tilde{s}\tilde{b}_1^*$ process and we have imposed $m_{\tilde{g}} \gtrsim 500$ GeV. The gluino-pair production process, which is also independent of $\sin^2\theta_m$, is only 2.9 fb, and only becomes relevant for $m_{\tilde{s}\tilde{b}_1} \gtrsim 300$ GeV. The branching ratio of the $\tilde{s}\tilde{b}_1$ into a b quark, however, scales as $\sin^2\theta_m$. We therefore give results for $\sin^2\theta_m = 1, 0.75, 0.5, 0.25$, and for 0, 1, and 2 b -tagged jet events. The case for $\sin^2\theta_m = 1$ is the same as a standard \tilde{b} squark.

We see that, for $\sin^2\theta_m \gtrsim 0.5$, if we only require at least one b -tagged jet rather than demanding double-tag, the cross section does not change drastically as $\sin^2\theta_m$ decreases from 1 to 0.5. Requiring a minimum of 10 signal events⁶ as suggestive evidence for such a squark, with an integrated luminosity of 2 fb^{-1} the sensitivity is around 300 GeV, if $\sin^2\theta_m \gtrsim 0.5$. If the integrated luminosity can go up to 20 fb^{-1} , then the sensitivity increases to 350 GeV.

We emphasize that the double-tag vs single-tag ratio contains information on $\sin^2\theta_m$, while their sum, when compared with the standard \tilde{b} squark pair production, provides additional consistency check on cross section vs mass. Such work would depend on more detailed knowledge of the detector, which we leave to the experimental groups.

V. DISCUSSION AND CONCLUSION

In this work, we have considered the SUSY scenario that the only light degrees of freedom are the right-handed strange-beauty squark ($m_{\tilde{s}\tilde{b}_1} \gtrsim 200$ GeV) and gluino ($m_{\tilde{g}} = 500$ GeV). Such a light squark is a result of a near-maximal mixing in the 2-3 sector of the right-handed squarks, which is in turn a result of approximate Abelian flavor symmetry.

We have performed calculations for direct strange-beauty squark-pair production, as well as the feed down from gluino-pair production and the associated production of $\tilde{s}\tilde{b}_1$ with gluino. It turns out that the dominant contribution comes from direct squark-pair production as long as the

squark mass is below 300 GeV. As one has to require $m_{\tilde{g}} \gtrsim 500$ GeV, which comes from low energy bounds, gluino pair production is in general subdominant. However, as the squark mass is above 300 GeV, the feed down from gluino-pair production with $m_{\tilde{g}} = 500$ GeV becomes sizable. Furthermore, many new avenues such as $s\bar{s} (ss) \rightarrow \tilde{s}\tilde{b}_1\tilde{s}\tilde{b}_1^{(*)}$ opens up. These are, however, very suppressed at Tevatron energies because of heavy gluino mass.

We have studied three decay scenarios of the strange-beauty squarks that are relevant for the search at the Tevatron, which is of immediate interest because it can be readily done in the near future. The three decay modes that we have considered are (i) (quasi)stable $\tilde{s}\tilde{b}_1$ as in $\tilde{s}\tilde{b}_1$ -LSP SUSY or in gauge-mediated SUSY breaking with a very large \sqrt{F} , (ii) R -parity violating decay of $\tilde{s}\tilde{b}_1$ (hence $\tilde{s}\tilde{b}_1$ behaves like a leptoquark), and (iii) the popular case of $\tilde{s}\tilde{b}_1 \rightarrow s/b\tilde{\chi}_1^0$ decay, where $\tilde{\chi}_1^0$ is the LSP. In the first case, the $\tilde{s}\tilde{b}_1$ once produced would hadronize into a massive stable charged particle like a ‘‘heavy muon,’’ which would ionize and form a track in the central tracking system and in the outer muon chamber. This is a very clean signature. The sensitivity for run II with an integrated luminosity of 2 fb^{-1} is up to about 300 GeV, which may increase to about 350 GeV with an order more luminosity. In the second case, the $\tilde{s}\tilde{b}_1$ decays like a leptoquark of the first or second generation. The best current limit is 260 GeV (preliminary [16]) for the first generation. This is already at the sensitivity level of the Tev2000 study [17] for 2 fb^{-1} . With an order more luminosity, the limit should reach 350 GeV. In the last case, $\tilde{s}\tilde{b}_1 \rightarrow s/b\tilde{\chi}_1^0$ decay leads to multiple b -jets plus large missing energy in the final state. The number of b -tag events depends on the mixing angle $\sin\theta_m$, because the branching ratio of $\tilde{s}\tilde{b}_1 \rightarrow b\tilde{\chi}_1^0$ scales as $\sin^2\theta_m$. As long as $\sin^2\theta_m \gtrsim 0.5$, the sensitivity at the run II with 2 fb^{-1} goes up to about 300 GeV. With improved b -tagging in run II, one can also make use of the single versus double b -tag ratio as well as the b -tagged cross section to determine $m_{\tilde{s}\tilde{b}_1}$ and the mixing angle $\sin^2\theta_m$.

At the LHC $\tilde{s}\tilde{b}_1\tilde{s}\tilde{b}_1^*$ and $\tilde{g}\tilde{g}$ pair production cross sections are comparable, with gg fusion being the dominant mechanism. Unlike at the Tevatron, the associated production of $sg \rightarrow \tilde{s}\tilde{b}_1\tilde{g}$ becomes interesting at the LHC. Nevertheless, $\tilde{s}\tilde{b}_1\tilde{s}\tilde{b}_1$ or $\tilde{s}\tilde{b}_1^*\tilde{s}\tilde{b}_1^*$ pair production remains relatively unimportant. With $\tilde{s}\tilde{b}_1$ as light as 200 GeV, $\tilde{s}\tilde{b}_1\tilde{s}\tilde{b}_1^*$ pair production may be relatively forward. On the other hand, $\tilde{g}\tilde{g}$ events, followed by $\tilde{g} \rightarrow \tilde{s}\tilde{b}_1\bar{s}/\bar{b}$, would have extra hard jets to provide more handles. The $\tilde{s}\tilde{b}_1\tilde{g}$ final state, if it can be separated, can probe the mixing angle $\cos^2\theta_m$ in the production cross section. Discovery of the strange-beauty squark at the LHC should be no problem at all, but the richness demands a more dedicated study, which we leave for future work.

In conclusion, the recent possible CP violation discrepancy in $B \rightarrow \phi K_S$ decay suggests the possibility of a light strange-beauty squark $\tilde{s}\tilde{b}_1$ that carries both strange and beauty flavors. Such an unusual squark can be searched for at

⁶From an experimental study of scalar bottom quark search by CDF [18], the background comes from $t\bar{t}$, single and pair vector boson production. Using b -tagging the number of background events was reduced to the few events level with run I data. Therefore, with ten times more luminosity in run II but much improved b -tagging and event selection techniques, the background should be of $\mathcal{O}(10)$ events. If so, 10 signal events above this background would have a sensitivity of 2 sigma or more. So, for simplicity we use 10 signal events as a rough criteria for sensitivity reach.

the Tevatron run II, with the precaution that $\widetilde{s\bar{b}}_1$ can decay into a beauty or strange quark, and the standard \bar{b} search should be broadened. Discovery up to 300 GeV is not a problem, and anomalous behavior in both production cross sections and the single versus double tag ratio may provide confirming evidence for the strange-beauty squark.

ACKNOWLEDGMENT

This research was supported in part by the National Science Council of Taiwan R.O.C. under grant no. NSC 92-2112-M-007-053- and NSC-92-2112-M-002-024, and by the MOE CosPA project.

-
- [1] Y. Nir and N. Seiberg, Phys. Lett. B **309**, 337 (1993); M. Leurer, Y. Nir, and N. Seiberg, Nucl. Phys. **B420**, 468 (1994).
 [2] C.K. Chua and W.S. Hou, Phys. Rev. Lett. **86**, 2728 (2001).
 [3] A. Arhrib, C.K. Chua, and W.S. Hou, Phys. Rev. D **65**, 017701 (2002).
 [4] Belle Collaboration, K. Abe *et al.*, Phys. Rev. D **67**, 031102 (2003).
 [5] Belle Collaboration, K. Abe *et al.*, Phys. Rev. Lett. **91**, 261602 (2003).
 [6] T. Browder, Int. J. Mod. Phys. A **19**, 965 (2004).
 [7] C.K. Chua, W.S. Hou, and M. Nagashima, Phys. Rev. Lett. **92**, 201803 (2004).
 [8] CDF Collaboration, T. Affolder *et al.*, Phys. Rev. Lett. **88**, 041801 (2002); “Higgs and Supersymmetry at collider experiments,” talk by M. Schmitt at the Lepton-Photon Symposium 2003, Fermilab, U.S.A.
 [9] W. Beenakker, R. Hopker, M. Spira, and P. Zerwas, Nucl. Phys. **B492**, 51 (1997); hep-ph/9611232.
 [10] Particle Data Group, K. Hagawara *et al.*, Phys. Rev. D **66**, 010001 (2002).
 [11] CDF Collaboration, F. Abe *et al.*, Phys. Rev. D **46**, R1889 (1992); CDF Collaboration, A. Connolly, hep-ex/9904010; CDF Collaboration, K. Hoffman, hep-ex/9712032.
 [12] CDF Collaboration, D. Acosta *et al.*, Phys. Rev. Lett. **90**, 131801 (2003).
 [13] H. Baer, K. Cheung, and J. Gunion, Phys. Rev. D **59**, 075002 (1999).
 [14] K. Cheung and G. Cho, Phys. Rev. D **67**, 075003 (2003); **69**, 017702 (2004).
 [15] J. Feng and T. Morii, Phys. Rev. D **58**, 035001 (1998).
 [16] CDF Collaboration, F. Abe *et al.*, Phys. Rev. Lett. **79**, 4327 (1997); **81**, 4806 (1998). The latest preliminary results from CDF is available at <http://www-cdf.fnal.gov/physics/exotic/exotic.html>; $D\bar{0}$ Collaboration, V.M. Abazov *et al.*, Phys. Rev. D **64**, 092004 (2001); B. Abbott *et al.*, Phys. Rev. Lett. **84**, 2088 (2000). The latest preliminary results from $D\bar{0}$ is available at <http://www-d0.fnal.gov/Run2Physics/np/>.
 [17] D. Amidei *et al.*, “Future Electroweak Physics at the Fermilab Tevatron,” Report of the tev_2000 Study Group, Fermilab-Pub-96/082, 1996.
 [18] CDF Collaboration, T. Affolder *et al.*, Phys. Rev. Lett. **84**, 5704 (2000).